



Characterization of Atmospheric Ekman Spirals at Dome C, Antarctica

Jean-François Rysman, Alain Lahellec, Etienne Vignon, Christophe Genthon,
Sébastien Verrier

► To cite this version:

Jean-François Rysman, Alain Lahellec, Etienne Vignon, Christophe Genthon, Sébastien Verrier. Characterization of Atmospheric Ekman Spirals at Dome C, Antarctica. *Boundary-Layer Meteorology*, 2016, 160 (2), pp. 363-373. 10.1007/s10546-016-0144-y . hal-01306757

HAL Id: hal-01306757

<https://hal.sorbonne-universite.fr/hal-01306757>

Submitted on 25 Apr 2016

HAL is a multi-disciplinary open access archive for the deposit and dissemination of scientific research documents, whether they are published or not. The documents may come from teaching and research institutions in France or abroad, or from public or private research centers.

L'archive ouverte pluridisciplinaire **HAL**, est destinée au dépôt et à la diffusion de documents scientifiques de niveau recherche, publiés ou non, émanant des établissements d'enseignement et de recherche français ou étrangers, des laboratoires publics ou privés.

Characterization of atmospheric Ekman spirals at Dome C, Antarctica

Jean-François Rysman · Alain Lahellec · Etienne

Vignon · Christophe Genthon · Sébastien Verrier

Abstract We use wind speed and temperature measurements taken along a 45-m meteorological tower located at Dome C, Antarctica (75.06 °S, 123.19 °E) to highlight and characterize the Ekman spiral. Firstly, temperature records reveal that the atmospheric boundary layer at Dome C is stable during winter and summer nights (i.e., > 85 % of the time). The wind vector also shows a strong dependence in speed and direction with elevation. The Ekman model was then fitted to the measurements. Results show that the wind vector followed the Ekman spiral structure for more than 20 % of the year 2009. Most Ekman spirals have been detected during summer nights, that is, when the boundary layer is slightly stratified. During these episodes, the boundary-layer height ranged from 25 to 100 m, eddy viscosity coefficient from 0.004 to 0.06 m² s⁻¹, and the Richardson number from 0 to 1.6.

Keywords Atmospheric boundary layer · Dome C · Ekman spiral · Meteorological tower

1 Introduction

The Antarctic plateau is the coldest and one of the driest places on Earth (King and Turner, 1997). The flatness of this ice-covered desert with altitude ranging from 2000 to 4000 m, along with its extreme climatic conditions, makes it an exceptional setting for meteorological observations, particularly for the study of the atmospheric boundary layer. The Antarctic Plateau boundary layer is extremely stable and shallow during a large part of the year (Connolley, 1996; Hudson and Brandt, 2005; Hagelin et al.,

JF Rysman
Laboratoire de Météorologie Dynamique, IPSL, CNRS, Ecole Polytechnique, France E-mail: jfrysman@lmd.polytechnique.fr

A Lahellec
Laboratoire de Météorologie Dynamique, IPSL, UPMC Univ. Paris 06, France

E Vignon
Université Grenoble Alpes / CNRS Laboratoire de Glaciologie et Géophysique de l'Environnement (LGGE), France

C Genthon
Université Grenoble Alpes / CNRS Laboratoire de Glaciologie et Géophysique de l'Environnement (LGGE), France

S Verrier
LOCEAN (UPMC/IPSL), CNES, France

2008; Genthon et al., 2013) but can be convective on summer days, e.g., at Dome C (Mastrantonio et al., 1999; Georgiadis et al., 2002; Argentini et al., 2005; King et al., 2006; Genthon et al., 2010; Pietroni et al., 2012; Casasanta et al., 2014). Yet, because of the extreme conditions encountered in Antarctica, long-term and steady measurements are rare and the Antarctic Plateau boundary layer is still not yet fully characterized and understood (i.e., the role of the Coriolis effect in very stable regimes, the parametrization and modelling of the long-lived stable boundary layer in winter (Pietroni et al., 2012)).

One consequence of a neutral or stable boundary layer is the dependence of wind speed and direction on the elevation. Ekman (1905) developed, initially for the oceanic boundary layer and then adapted to the atmosphere, a theoretical model to explain the vertical wind profile. Specifically, Ekman (1905) showed that, in a neutral boundary layer, flow is constrained by pressure forces, Coriolis forces, and the divergence of turbulent fluxes of momentum resulting in the well-known Ekman spiral. However, the conditions for Ekman spirals (no baroclinicity, no topographic effects, steady state, static neutrality and no subsidence) are very seldom met in the atmosphere, although they are frequent in the ocean. As a result, very little evidence of the Ekman spiral has emerged for the atmosphere, e.g., at Leipzig (Germany) (Mildner, 1950; Lettau, 1950), at Cabauw (the Netherlands) (Van Ulden and Wieringa, 1996), in the Arctic (Grachev et al., 2005), and in Antarctica (Mahrt and Schwerdtfeger, 1970; Kuhn et al., 1977; Lettau et al., 1977; Kottmeier, 1986). More recently, Genthon et al. (2010) mentioned the night time occurrences of the Ekman spiral at Dome C on the Antarctic plateau, this location meeting the conditions for the frequent occurrence of Ekman spirals. Indeed, the Dome C is located on a very flat plateau with a slope $< 1 \times 10^{-3}$. This region is isolated and rarely affected by atmospheric perturbations, allowing a steady-state and barotropic atmosphere, with summer nights favorable to neutral or slightly stratified boundary layers. Finally, very few attempts to estimate the subsidence at Dome C has been done so far (Argentini et al., 2005; Pietroni et al., 2012) and the occurrence and intensity of subsidence at Dome C is still an open question.

The observation and characterization of the atmospheric Ekman spiral around the world are worthwhile in terms of evaluating the turbulence parametrizations of climate models. Indeed, Sandu et al. (2014) and Holtslag et al. (2013) describe the current problem of modelling the stable boundary layer, showing a global tendency of models to both overestimate the surface drag that leads to an excessively deep boundary layer, and to underestimate wind rotation with height in the lower atmosphere. Therefore our study aims at providing a detailed characterization of the Ekman spiral at Dome C, including the estimation of the eddy viscosity coefficient. To this aim, we used wind and temperature observations collected between January and December 2009 at a meteorological tower located at Dome C.

Section 2 presents the geographical settings of Dome C and the characteristics of the measurements, with the Ekman model and method of analysis presented in Sect. 3. Section 4 is dedicated to the results. Firstly, we characterize the atmospheric stability at Dome C that results in the strong vertical dependence of the wind vector. We then identify conditions under which the Ekman model fitted the wind profiles in 2009 before evaluating and discussing the associated parameters. The discussion is found in Sect. 5.

2 Geographical settings and measurements

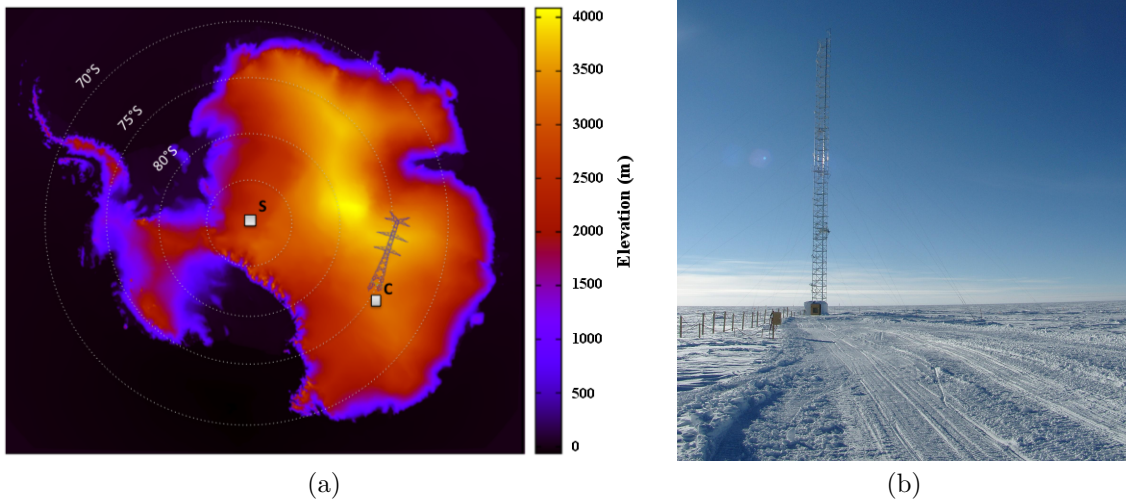


Fig. 1 (a) Map of Antarctica and the 45-m tower location (C): S symbolises the South Pole. (b) The instrumented tower.

Dome C is a local topographic maximum ($75^{\circ} 06' S$, $123^{\circ} 20' E$, 3233 m a.s.l.) of the Antarctic Plateau where the French-Italian Concordia scientific station has operated since 1997 (Fig. 1a). A 45-m meteorological tower was erected close to the station (Fig. 1b) on which temperature, humidity and wind measurements have been taken since 2008. In particular, in 2009, six Vaisälä thermo-hygrometers (four HMP155 and two HMP45AC), six platinum resistance thermometers in mechanically ventilated shields and six Young 45106 aerovanes were operated at heights of 3.6 m, 11 m, 18.6 m, 25.9 m, 33.2 m and 42.4 m (± 0.5 m). Measurements were taken with a 10-second timestep and averaged over 30 min. These measurements have already provided new insights into the Antarctic boundary layer (Genthon et al., 2010, 2013; Barral et al., 2014; Rysman et al., 2015).

3 Ekman spiral

3.1 The Ekman model

In the Ekman model, the wind vector rotates and increases in magnitude with elevation showing a spiral shape on the wind hodograph known as the Ekman spiral. The Ekman spiral results from the equilibrium between pressure forces, Coriolis forces and the divergence of turbulent fluxes of momentum. Theoretically, above a given height, the flow follows the large-scale atmospheric circulation. The Ekman model equations can be expressed as follows,

$$k_m \frac{\partial^2 \bar{u}}{\partial z^2} + f(\bar{v} - \bar{v}_g) = 0, \quad (1a)$$

$$k_m \frac{\partial^2 \bar{v}}{\partial z^2} - f(\bar{u} - \bar{u}_g) = 0, \quad (1b)$$

where f is the Coriolis parameter, k_m is the eddy viscosity coefficient taken to be constant vertically, u and v are the horizontal wind components within the boundary layer, and u_g and v_g are the large-scale wind components; the overbar corresponds to Reynolds averaging (see Holton (1992) for details). The wind components for the Southern Hemisphere are thus,

$$u = -u_g \cos(\gamma z) e^{-\gamma z} + v_g \sin(\gamma z) e^{-\gamma z} + u_g, \quad (2a)$$

$$v = -v_g \cos(\gamma z) e^{-\gamma z} - u_g \sin(\gamma z) e^{-\gamma z} + v_g, \quad (2b)$$

where $\gamma = (-f/2k_m)^{1/2}$. The Ekman height is usually defined as $h_{ek} = \pi/\gamma$ (Holton, 1992) and corresponds to the distance from the ground where surface drag becomes negligible. Use of the Ekman model to fit the measurements allows one to characterize the eddy viscosity coefficient, the large-scale wind and the boundary-layer height. Note that, as the eddy viscosity coefficient is height dependant in a stratified boundary layer, the Ekman model only fits wind profiles when the k_m coefficient does not vary significantly along the tower; the k_m value is thus an average value along the vertical.

3.2 Model fitting

To assess the validity of the Ekman model for characterizing the wind profile at Dome C, the Ekman model was fitted to each 30-min averaged wind profile using Eq. 2. The large-scale wind components were constrained to the $[-20:20] \text{ m s}^{-1}$ range. Moreover, as the accuracy of wind sensors is 0.3 m s^{-1} , we only retained wind measurements with speed exceeding 1 m.s^{-1} and ensured that at least four levels out of the available six met this requirement. The γ parameter range was set to take into account the

angular accuracy of the wind aero-vanes and constrained to [0.004:0.13], this constraint implies that the lowest Ekman height characterized by the tower is 24 m. The non-linear fitting has been performed using the Levenberg-Marquardt algorithm (Levenberg et al., 1944).

Assessing whether the Ekman model fits the measurements implies testing the consistency of several well-chosen variables with the expected probability distribution. In particular, we tested the residuals (r) (not shown in the following) and the quadratic error (Q^2) distributions. Residuals are thus defined as,

$$r_i = y_i - f(x_i) \quad (3)$$

where $i = 1...n$ is associated with n measurements (12 in our analysis), y is a dependant variable (e.g., wind observation), f is the model function (e.g., Ekman model) and x is an independent (i.e., predictor) variable (e.g., altitude). The quadratic error is defined as,

$$Q^2 = \sum_{i=1}^n \frac{r_i^2}{\sigma^2} \quad (4)$$

where σ is the standard deviation (wind sensor accuracy). The data are assumed to follow a normal distribution and to be centered on the Ekman model, while the measurement errors are assumed to be independent and Gaussian with a zero mean. If the Ekman model is relevant for describing the wind profile in the Dome C boundary layer, then our fitted Q^2 distribution should have a χ^2 distribution with nine degrees of freedom (12 measurements – three parameters). This hypothesis is tested by computing the χ^2 probabilities defined as,

$$y = \int_{\chi^2}^{+\infty} \varphi(\chi'^2, n) d\chi'^2 \quad (5)$$

φ is a probability density function with n degrees of freedom, which follows a χ^2 distribution. If our fitted Q^2 distribution follows the χ^2 distribution with n degrees of freedom, then the y -distribution must be constant as a function of probability. To obtain such a distribution, the standard deviation has to be adjusted (see below).

4 Results

Figure 2 highlights the stability of the lower atmosphere at Dome C in 2009 (>85% of the year). From March to mid-October, the atmosphere is stable almost without interruption except during a period of sudden warming at the beginning of July. On some days (e.g., in early May) the stability is considerable, stratification exceeding 10 K between 42.4 m and 3.6 m. From January to February, and from November to December, the diurnal variability is large; the atmosphere is moderately stable at night and often

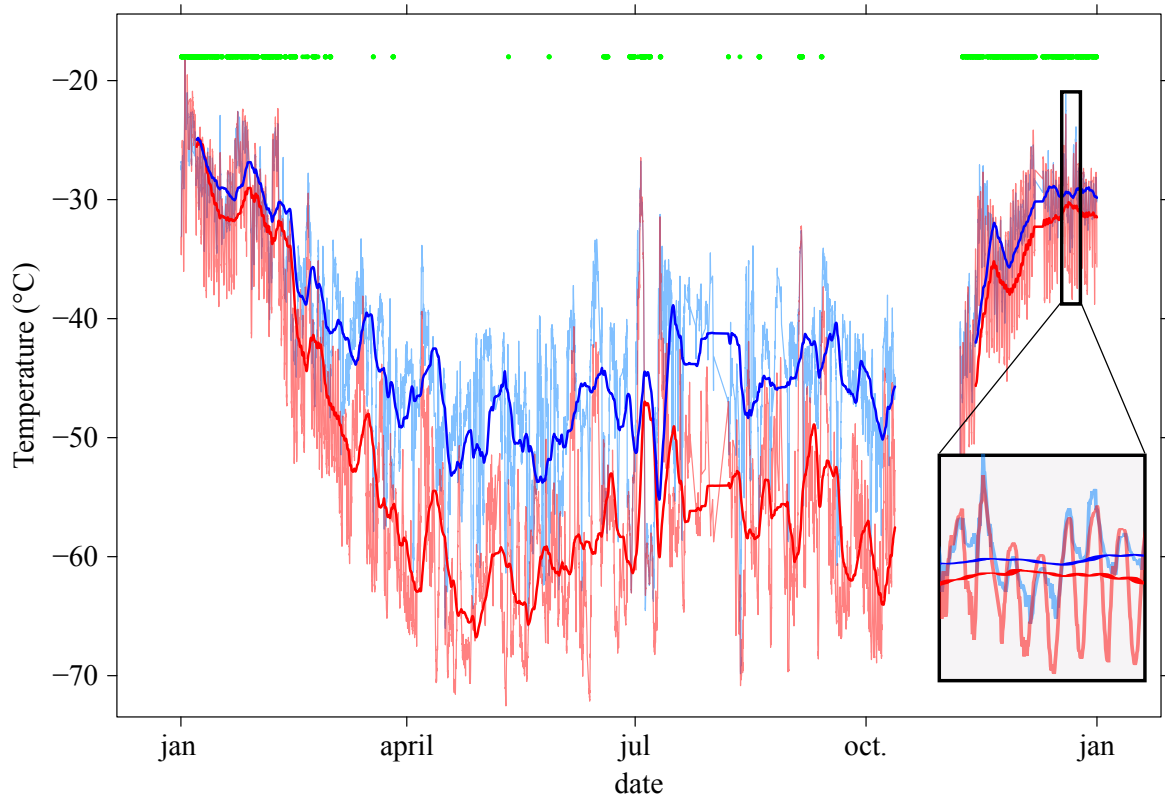


Fig. 2 Temperature for 3.6 m (shaded red) and 42.4 m (shaded blue) sensors in 2009. A six-day moving average temperature is displayed using red (3.6 m) and blue (42.4 m) lines. Green points indicate the episodes of convective boundary layer. A zoom is shown in the black box to highlight the diurnal cycle.

convective during the day. Further information about the seasonal cycle of temperature at Dome C can be found in Genton et al. (2013).

During summer, wind speed and direction are almost independent of altitude during daytime — when the sun is sufficiently high above the horizon, that is, from approximately 0900Z to 1800Z — but when the sun is low above the horizon, the atmosphere becomes very stratified. Figure 3 shows the wind hodograph for a typical summer afternoon (24 December). At 1200Z and 1500Z, the wind direction does not depend on height while the wind speed is very slightly dependent on height. From 1800Z onwards, a strong height dependence in speed appears (from 2.8 m s^{-1} at 3.6 m to 4.3 m s^{-1} at 42.4 m) but without height dependence in direction. At 2100Z, the wind is markedly stratified in terms of both speed (from 2.5 m s^{-1} at 3.6 m to 6.1 m s^{-1} at 42.4 m) and direction (from 46.5° at 3.6 m to 9.5° at 42.4 m). This stratification results in an Ekman spiral-like structure.

Therefore, since the atmosphere exhibited a neutral and stable temperature stratification at Dome C for more than 85 % of the calendar year 2009, with numerous wind observations showing a rotation and increase with height, we tested the validity of the Ekman model (Eq. 2). Firstly, as explained in Sect. 3.2, the standard deviation (i.e., the wind sensor accuracy provided by the manufacturer) was adjusted to

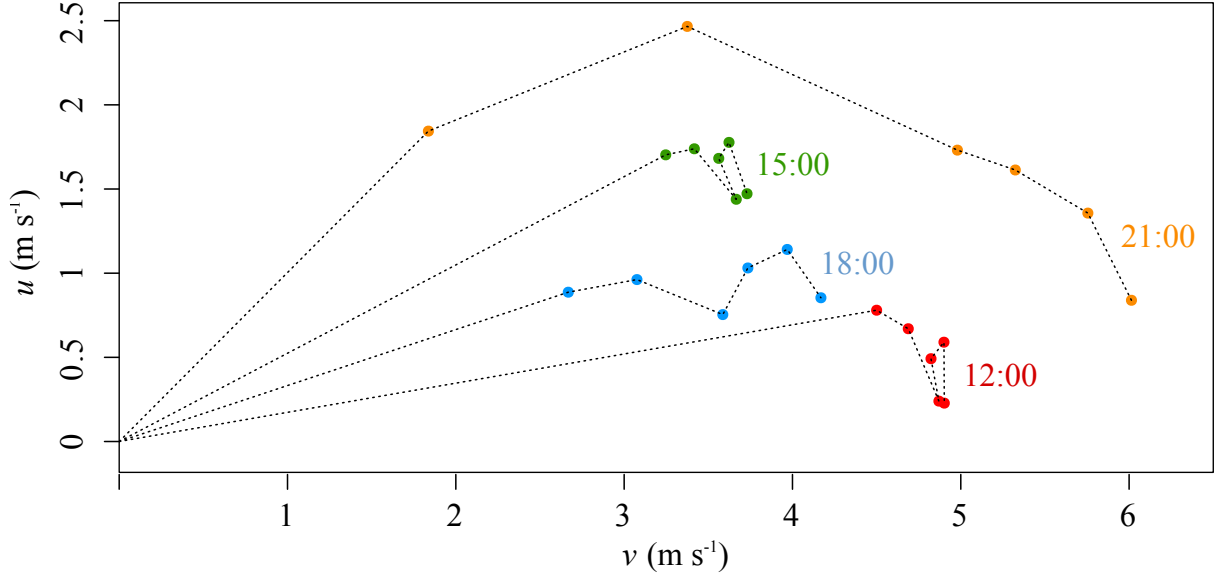


Fig. 3 Wind hodograph as a function of time on 24 December 2012.

obtain a constant y -distribution (Eq. 5). This showed that we needed to increase the standard deviation σ by a factor of 2.5 to account for the extreme climatic conditions of the Antarctic region as well as the turbulent wind fluctuations. Taking this correction into account, we found that during at least 20 % of the year 2009 (24 % of neutral and stable conditions), the wind profile followed an Ekman spiral pattern (Fig. 4). The vast majority of Ekman spirals were observed from January to mid-March, and from mid-November to December, i.e., approximately when the diurnal cycle is significant at Dome C. Fig. 2 shows that very few Ekman spirals are detected when the temperature is extremely low (especially from mid-April to the end of May), while several Ekman spirals are detected when the temperature is higher (e.g., in June).

Figure 5 highlights the occurrence of Ekman spirals and the corresponding Ekman-layer height in late December 2009. We also plotted the bulk Richardson number (R_i) between the highest and lowest levels of the tower, defined as,

$$R_i = \frac{\frac{g}{\theta_v} \frac{\Delta \bar{\theta}_v}{\Delta z}}{\frac{\Delta \bar{U}^2}{\Delta z} + \frac{\Delta \bar{V}^2}{\Delta z}} \quad (6)$$

where θ_v is the virtual potential temperature. Figure 5 emphasises that the Ekman model fits the wind during the night, i.e., when the atmosphere is slightly stable and the Richardson number slightly positive. During these episodes, the Ekman height ranges from 30 to 60 m. Figure 5 also shows that, as the Richardson number increases during the night (associated with increasing temperature stratification), the Ekman height decreases. Moreover, this figure also highlights that when the Richardson number is high (>3), and thus when turbulence is confined very close to the surface, the wind profile does not present an Ekman spiral structure. Note that free convection and extreme stable stratification episodes

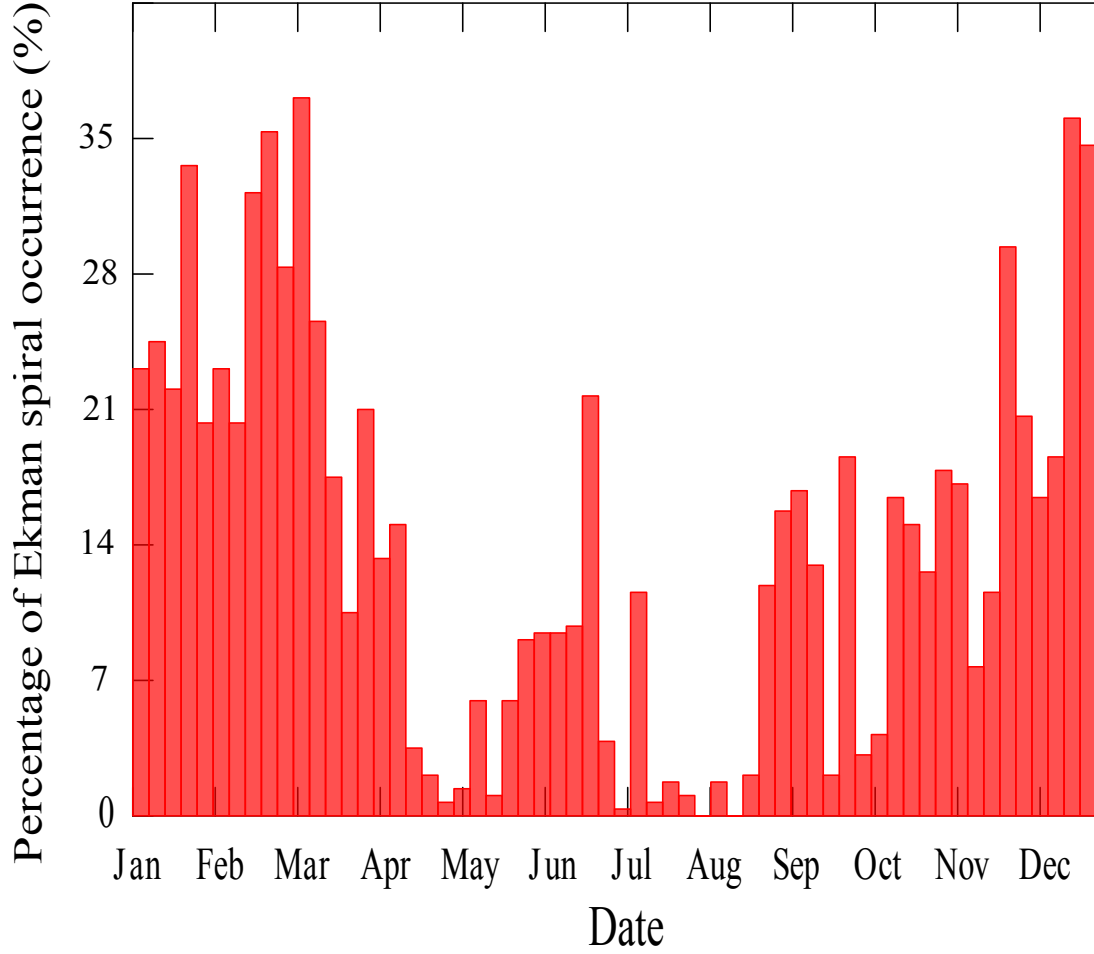


Fig. 4 Percentage Ekman spirals occurring over 6-day periods during the year 2009. 50% indicates that Ekman spirals occurred during half of a given 6-day period. Note the Ekman spiral structure cannot be detected with the tower when the atmospheric boundary layer depth is lower than 24 m.

highlighted by the negative and strongly positive values of R_i are associated to very small difference in temperature and/or in wind between top and bottom of the tower and are thus subject to high incertitude given the limited accuracy of wind and temperature sensors.

Figure 6 presents a normalized Ekman spiral i.e., $(\sqrt{u_g^2 + v_g^2} - \sqrt{v^2 + u^2})/\sqrt{u_g^2 + v_g^2}$ as a function of z/h_{ek} when the Ekman model fits the wind profiles. This figure shows that the 42.4-m sensor and even the 33.2-m sensor are sometimes found above the Ekman height. The normalized Ekman spiral also shows that the 18.6-m sensor sometimes show null wind speed and that the 3.6-m wind speed is, most of the time, over estimated by the Ekman model. Both features can also be observed in the analysis of residuals (not shown). It is not surprising that most of the time, the wind speed at 3.6 m is higher than the value predicted by the Ekman model because, close to the ground, in the atmospheric surface layer, the viscosity coefficient varies sharply when it is assumed constant in the Ekman model. This result supports the hypothesis that the surface-layer height lies between 3 and 10 m for the fitted case.

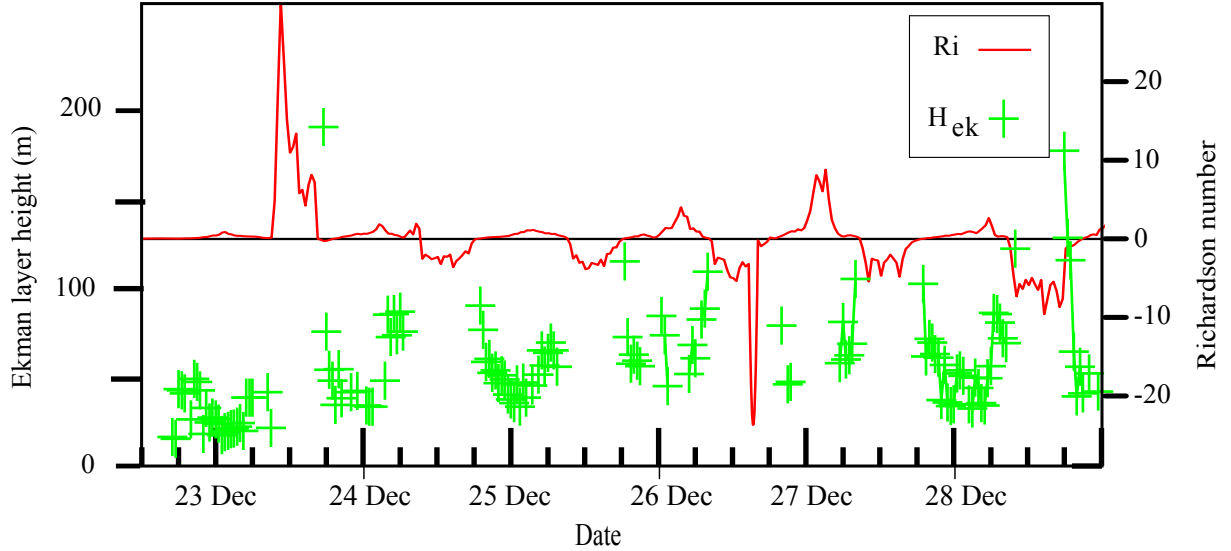


Fig. 5 Richardson number (red) and Ekman height (green) when the wind profile follows the Ekman spiral model. Note that free convection and extreme stable stratification episodes highlighted by the negative and strongly positive values of R_i are associated to very small difference in temperature and/or in wind between top and bottom of the tower and are thus subject to high uncertainty given the limited accuracy of wind and temperature sensors.

When the Ekman model fits the wind profile (i.e., mainly during summer nights), the boundary-layer height mostly ranges between 25 and 100 m, which is in agreement with previous studies (King et al., 2006; Pietroni et al., 2012). This value can be placed into perspective since on convective days the boundary-layer height can reach 200-350 m (Aristidi et al., 2005; Argentini et al., 2005; King et al., 2006).

The eddy viscosity coefficient characterizes the transport and dissipation of energy in the flow. The fit shows that this coefficient mainly ranges between 0.004 and $0.06 \text{ m}^2 \text{ s}^{-1}$, that is, two orders of magnitude lower than the typical value at mid-latitudes for a stable layer. The Richardson number mostly ranges between zero and 1.6 when the wind profile follows the Ekman model, i.e., in a neutral or slightly stratified boundary layer.

5 Discussion and conclusion

We have highlighted and characterized a significant number of atmospheric Ekman spirals during the 2009 campaign at Dome C, Antarctica. Specifically, we analyzed wind and temperature measurements using aero-vanes and thermometers deployed along a 45-m tower. We showed that the boundary layer was neutral or stable during 85 % of the year. Ekman spirals were detected for at least 20 % of the time series (i.e., more than 52 days in total) mainly during summer “nights” (i.e., with low solar elevation above the horizon). This analysis also revealed that the Ekman height mostly ranges between 25 and 100 m, much shallower than for the mid-latitude boundary layer. We found that, when the Ekman model fits the wind profile, the eddy viscosity coefficient ranges between 0.004 and $0.06 \text{ m}^2 \text{ s}^{-1}$, while the bulk

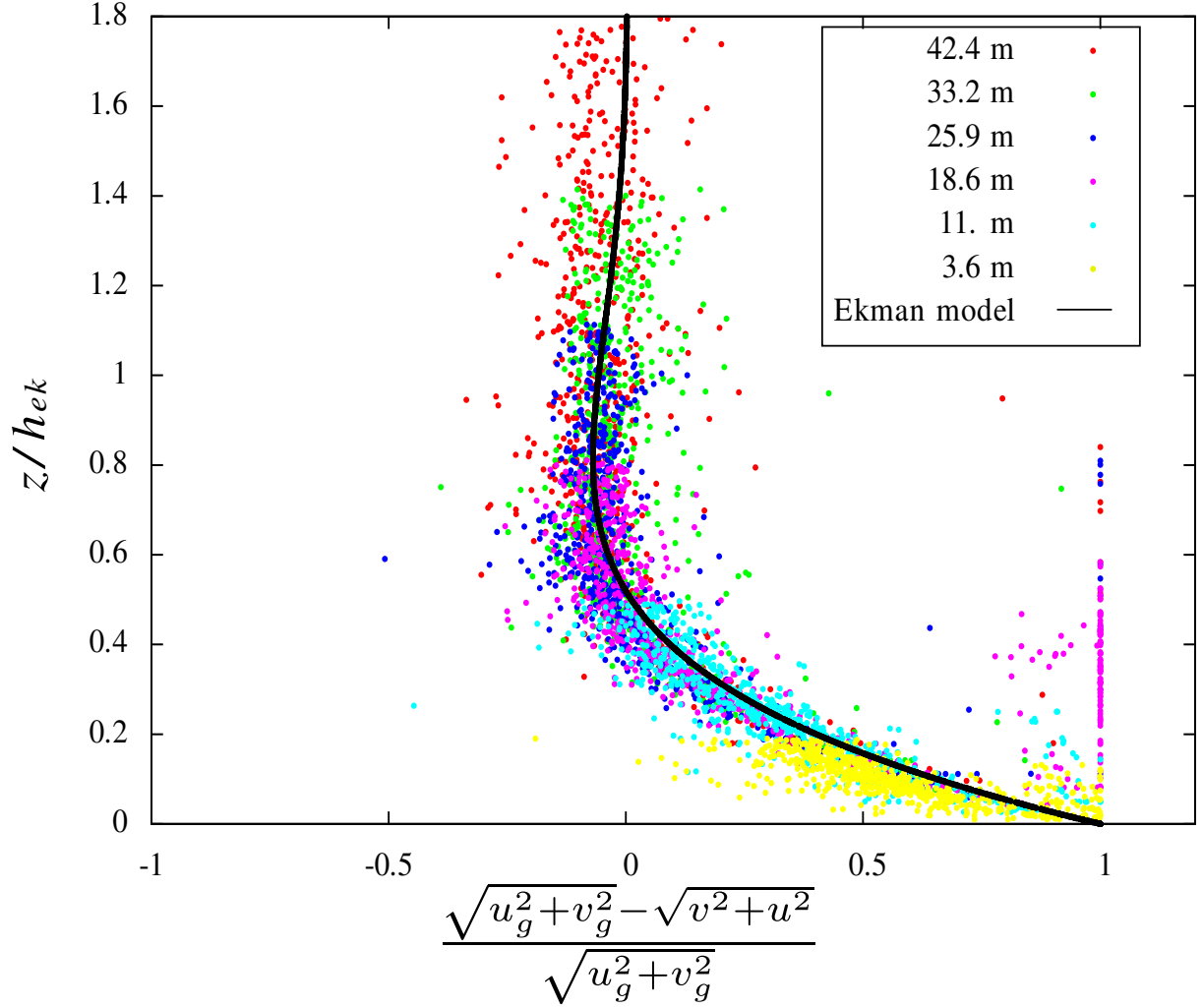


Fig. 6 Normalized Ekman spiral when the Ekman model fits the wind profiles per sensor. The thick black line shows the Ekman model relation.

Richardson number mainly ranges between zero and 1.6, implying that the boundary layer is neutral or slightly stratified.

Using measurements from a similar tower located on the Arctic sea-ice, Grachev et al. (2005) defined four regimes for the stable boundary layer that depend on the turbulence characteristics, the boundary layer stability and the influence of the Earth’s rotation. Our results show that, when the Ekman model fits the observations, the boundary layer is in the so-called “turbulent Ekman layer” regime (when $R_i \leq R_{ic} \approx 0.2$, where R_{ic} is the critical Richardson number) and in the “intermittently turbulent Ekman layer” regime (or supercritical stable regime) (when $R_i \geq R_{ic} \approx 0.2$). In complete accordance with our results, Grachev et al. (2005) argued that, for these regimes, the surface layer is very shallow and the wind profile is influenced by the Coriolis force, with some Ekman-spiral-like features being observed. Specific parametrizations associated with these regimes that take into account the Coriolis effect are certainly needed especially in models with coarse vertical resolution.

It must also be emphasized that nearly 80 % of wind profiles were not adjusted to the Ekman model. In particular, we showed that the Ekman model fitted the data rarely in winter. Several explanations can be put forward. First, the aero-vanes are rarely monitored in winter due to the harsh meteorological conditions and thus the extreme temperatures and frost deposition affect measurement availability and accuracy. Moreover, the reduced number of Ekman spiral detected in winter is also related to the very strong stability often found during this season, in contradiction to the condition of static neutrality of the Ekman model. This is consistent with the Richardson number lying between zero and 1.6 when the Ekman model fits the wind profile measurements, implying that Ekman spirals only develop within a “slightly” (regarding average stability conditions at Dome C) stratified boundary layer for which eddy viscosity coefficient does not vary significantly along the vertical. Occasional meteorological events can also prevent the development of Ekman spirals such as the occurrence of nocturnal jets (Gallée et al., 2015b) or subsidence (Argentini et al., 2005; Pietroni et al., 2012). Last but not least, seasonal conditions can prevent the tower from characterizing the boundary layer. In the winter, the boundary layer can be too shallow (only few tens of metres, Pietroni et al. (2012); Gallée et al. (2015a)) to be characterized by the tower (i.e., lower than 24 m (see Sect. 3.2)) while, in the summer, the boundary layer can be too deep.

Overall, this analysis provides new insights into the characteristics of the boundary layer, which could be used for model parametrizations (e.g., eddy viscosity and Ekman height). Pietroni et al. (2012) stressed the difficulty of defining the boundary-layer height in stable cases because its definition is often based on available measurements rather than on theory. Therefore, our method, with its clear physical background, could be applied for neutral and slightly stratified boundary layers at Dome C. Moreover, Pietroni et al. (2012) evaluated several boundary-layer height parametrizations at Dome C. They showed that the one proposed in Zilitinkevich (2002); Zilitinkevich et al. (2007) is the most accurate estimation of boundary-layer height at Dome C. In this parametrization, the boundary-layer height equals the Ekman-layer height when the atmosphere is neutral (see Eq. 3 from Zilitinkevich et al., 2007). This highlights the relevance of using Ekman model for estimating the boundary-layer height in neutral or slightly stratified boundary layer at Dome C.

Further analyses using this and subsequent datasets are needed to estimate the Ekman pumping and the associated subsidence. Moreover as the measurements at Dome C tower are still on-going, information about the seasonal and inter-annual variability of the boundary layer will be available and could be used to detect possible changes in climatic conditions at Dome C in the context of the global warming.

Acknowledgements We would like to thank Jean-Yves Grandpeix for his valuable help for the statistical analysis and Chantal Claud for her support that allows to achieve this paper. Boundary layer observation and research at Dome C

were supported by the French Polar Institute (IPEV; CALVA program), the Institut National des Sciences de l'Univers (Concordia and LEFE-CLAPA programs), the Observatoire des Sciences de l'Univers de Grenoble (OSUG) and the École Doctorale 129 - Sciences de l'environnement. We would like to thank the two anonymous referees and the editors Evgeni Fedorovich and John R. Garratt for their helpful comments, suggestions and editing.

References

- Argentini S, Viola A, Sempreviva AM, Petenko I (2005) Summer boundary-layer height at the plateau site of Dome C, Antarctica. *Boundary-Layer Meteorol* 115:409–422, DOI 10.1007/s10546-004-5643-6
- Aristidi E, Agabi K, Azouit M, Fossat E, Vernin J, Travouillon T, Lawrence JS, Meyer C, Storey JWV, Halter B, Roth WL, Walden V (2005) An analysis of temperatures and wind speeds above Dome C, Antarctica. *Astron Astrophys* 430:739–746, DOI 10.1051/0004-6361:20041876
- Barral H, Vignon E, Bazile E, Traullé O, Gallée H, Genthon C, Brun C, Couvreur F, Le Moigne P (2014) Summer diurnal cycle at Dome C on the Antarctic Plateau. 21st Symposium on Boundary Layer and Turbulence.
- Casasanta G, Pietroni I, Petenko I, Argentini S (2014) Observed and modelled convective mixing-layer height at Dome C, Antarctica. *Boundary-Layer Meteorol* 151:587–608, doi:10.1007/s10546-014-9907-5
- Connolley WM (1996) The Antarctic temperature inversion. *Int J Climatol* 16:1333–1342
- Ekman VW (1905) On the influence of the Earth's rotation on ocean currents. *Ark Mat Astron Fys* 2:1–53
- Gallée H, Barral H, Vignon E, Genthon C (2015) A case study of a low level jet during OPALE. *Atmos Chem Phys Discussion* 14:31,091–31,109, DOI 10.5194/acp-15-1-2015
- Gallée H, Preunkert S, Argentini S, Frey MM, Genthon C, Jourdain B, Pietroni I, Casasanta G, Barral H, Vignon E, Legrand M, Amory C (2015) Characterization of the boundary layer at Dome C (East Antarctica) during the OPALE summer campaign. *Atmos Chem Phys* 15:6225–6236, DOI 10.5194/acp-15-6225-2015
- Genthon C, Town MS, Six D, Favier V, Argentini S, Pellegrini A (2010) Meteorological atmospheric boundary layer measurements and ECMWF analyses during summer at Dome C, Antarctica. *J Geophys Res Atmos* 115:D05104, DOI 10.1029/2009JD012741
- Genthon C, Gallée H, Six D, Grigioni P, Pellegrini A (2013) Two years of atmospheric boundary layer observation on a 45-m tower at Dome C on the Antarctic plateau. *J Geophys Res Atmos* pp 3218–3232, DOI 10.1002/jgrd.50128
- Georgiadis T, Argentini S, Mastrantonio G, Sozzi AVR, Nardino M (2002) Boundary layer convective-like activity at Dome Concordia, Antarctica. *Nuovo Cimento C Geophysics Space Physics C* 25:425

- Grachev AA, Fairall CW, Persson POG, Andreas EL, Guest PS (2005) Stable boundary-layer scaling regimes: The Sheba data. *Boundary-Layer Meteorol* 116:201–235, DOI 10.1007/s10546-004-2729-0
- Hagelin S, Masciadri E, Lascaux F, Stoesz J (2008) Comparison of the atmosphere above the South Pole, Dome C and Dome A: first attempt. *Mon Not R Astron Soc* 1510:1499–1510, DOI 10.1111/j.1365-2966.2008.13361.x
- Holton J (1992) An introduction to dynamic meteorology, Academic Press, San Diego, U.S.A, 511 pp.
- Holtstlag AAM, Svensson G, Baas P, Basu S, Beare B, Beljaars ACM, Bosveld FC, Cuxart J, Lindvall J, Steeneveld GJ, Tjernström M, Van de Wiel BJH (2013) Stable boundary layers and diurnal cycles. *Bull Amer Meteorol Soc* 94:1691–1706
- Hudson SR, Brandt RE (2005) A Look at the Surface-Based Temperature Inversion on the Antarctic Plateau. *J Clim* 18:1673–1696, DOI 10.1175/JCLI3360.1
- King JC, Turner J (1997) Antarctic meteorology and climatology. Cambridge University Press, UK, 409 pp
- King JC, Argentini SA, Anderson PS (2006) Contrasts between the summertime surface energy balance and boundary layer structure at Dome C and Halley stations, Antarctica. *J Geophys Res Atmos* 111:D02105, DOI 10.1029/2005JD006130
- Kottmeier C (1986) Shallow gravity flows over the Ekström ice shelf. *Boundary-Layer Meteorol.* 35(1-2):1–20
- Kuhn, M., Lettau, H., and Riordan, A. J. (1977) Stability Wind Spiraling in the Lowest 32 meters. in *Meteorological Studies at Plateau Station, Antarctica; Pap. 7, Antarctic Res. Ser. 25*, 93-I I I.
- Lettau, H. (1950) A reexamination of the “Leipzig wind profile” considering some relations between wind and turbulence in the frictional layer. *Tellus*, 2(2), 125–129.
- Lettau, H., Riordan, A., Kuhn, M. (1977). Air temperature and two-dimensional wind profiles in the lowest 32 meters as a function of bulk stability. *Meteorological studies at Plateau station, Antarctica*, J. A. Businger, Ed., Antarctic Research Series, Vol. 25, Amer. Geophys. Union, 77–91
- Levenberg, Kenneth (1944) A method for the solution of certain non-linear problems in least squares. *Quarterly of applied mathematics*, 2: 164–168
- Mahrt L, Schwerdtfeger W (1970) Ekman spirals for exponential thermal wind. *Boundary-Layer Meteorol* 1(2):137–145
- Mastrantonio G, Malvestuto V, Argentini S, Georgiadis T, Viola A (1999) Evidence of a convective boundary layer developing on the Antarctic plateau during the summer. *Meteorol Atmos Phys* 71:127–132, DOI 10.1007/s007030050050
- Mildner, P. (1932) Über die Reibung in einer speziellen Luftmasse in den untersten Schichten der Atmosphäre. *Beitr Phys freien Atmosphäre*. 19:151–158.

301 Pietroni I, Argentini S, Petenko I, Sozzi R (2012) Measurements and parametrizations of the atmo-
302 spheric boundary-layer height at Dome C, Antarctica. *Boundary-Layer Meteorol* 143:189–206, DOI
303 10.1007/s10546-011-9675-4

304 Rysman JF, Verrier S, Lahellec A, Genthon C (2015) Analysis of boundary-layer statistical properties
305 at Dome C, Antarctica. *Boundary-Layer Meteorol* pp 1–11

306 Sandu I, Beljaars A, Balsamo G (2014) Improving the representation of stable boundary layers. *ECMWF*
307 *Newsletter* 138:24–31

308 Van Ulden A, Wieringa J (1996) Atmospheric boundary layer research at Cabauw. In: *Boundary-Layer*
309 *Meteorol* 78:34–69

310 Zilitinkevich SS (2002) Third-order transport due to internal waves and non-local turbulence in the stably
311 stratified surface layer. *QJR Meteorol Soc* 128(581):913–925

312 Zilitinkevich S, Esau I, Baklanov A (2007) Further comments on the equilibrium height of neutral and
313 stable planetary boundary layers. *QJR Meteorol Soc* 133:265–271.